analytical chemistry

pubs.acs.org/ac Article

OLYMPIA-LILBID: A New Laboratory Setup to Calibrate Spaceborne Hypervelocity Ice Grain Detectors Using High-Resolution Mass Spectrometry

Arnaud Sanderink,* Fabian Klenner, Illia Zymak, Jan Žabka, Frank Postberg, Jean-Pierre Lebreton, Bertrand Gaubicher, Ales Charvat, Bernd Abel, Miroslav Polášek, Barnabé Cherville, Laurent Thirkell, and Christelle Briois

Cite This: *Anal. Chem.* 2023, 95, 3621−3628 Read Online

ACCESS | Metrics & More | Article Recommendations | Supporting Information

ABSTRACT: The coupling of an Orbitrap-based mass analyzer to the laser-induced liquid beam ion desorption (LILBID) technique has been investigated, with the aim to reproduce the mass spectra recorded by Cassini's Cosmic Dust Analyzer (CDA) in the vicinity of Saturn's icy moon Enceladus. LILBID setups are usually coupled with time-of-flight (TOF) mass analyzers, with a limited mass resolution (~800 $m/\Delta m$). Thanks to the Orbitrap technology, we developed a unique analytical setup that is able to simulate hypervelocity ice grains' impact in the laboratory (at speeds in the range of 15−18 km/s) with an unprecedented high mass resolution of up to 150 000 $m/\Delta m$ (at m/z 19 for a 500 ms signal duration). The results will be implemented in the LILBID database and will be useful for the calibration and future data interpretation of the Europa Clipper's SUrface Dust Analyzer (SUDA), which will characterize the habitability of Jupiter's icy moon Europa.

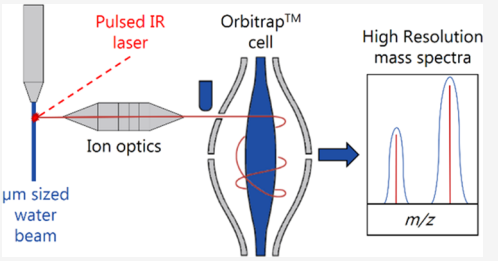

The search for extra-terrestrial life has always been a major endeavor in science, and has driven planetary exploration efforts since its debut. Planetary bodies with strong habitability potentials (*i.e.*, whether life could originate or be sustained on such bodies) are the target of many space missions.[1−4] In the search for life as we know it, liquid water is a mandatory prerequisite. This is why icy moons with subsurface oceans[5,6] in the outer solar system are such interesting bodies for astrobiology investigations. Among these moons, Europa and Enceladus, respectively, orbiting Jupiter and Saturn, are of particular interest because hydrothermal activity is believed to occur on their rocky sea floors.[7,8] Those liquid water oceans do show favorable conditions for the creation of a variety of organic molecules.[9−11] In the case of Enceladus[12] and potentially Europa,[13] gas, dust, and ice grains from the liquid ocean are emitted from the surface through plumes, allowing a study of the oceans composition from space by *in situ* instruments.[14−18] Mass spectrometers are amongst the most prevalent *in situ* instruments in space exploration. They enable the measurement of the samples' compositions, give access to their exact chemical formula, and reveal the complexity of their environments. They are specifically suitable to agnostically investigate the composition of organic materials. For this reason, they have flown onboard numerous probes toward a wide variety of solar system bodies, such as Venus,[19] Mars,[20] or smaller bodies like Saturn icy moon Titan[21] or the comet 67P/Churyumov-Gerasimenko.[22,23] On the latter mission, the instrument ROSINA was able to detect prebiotics chemicals, such as amino acids, in the coma of the comet.[24] Although mass spectrometry is an *in situ* technique, it does not necessarily require to land on the body or even to stay in its close vicinity. Hypervelocity impacts' detectors are able to sample emitted grains during spacecraft flybys, using the impact ionization technique, which generally starts to produce useful amounts of ions at impact velocities above 1−2 km/s.[25] As an example, the impact ionization mass spectrometer Cosmic Dust Analyzer[26] (CDA) on board the Cassini spacecraft was studied for 13 years around Saturn dust and ice grains emitted by Enceladus. By measuring the composition of μm-sized E-ring ice grains, it allowed characterizing Enceladus' ocean,[7,14,16] revealing a complex organic chemistry.[15,27,28] CDA could measure cationic mass spectra up to a mass to charge ratio (m/z) of ~230 with a mass resolution of 20−50 $m/\Delta m$,[26] where m is the mass of the ion and Δm is the full width at half maximum of the peak. The next generation of TOF hypervelocity detectors with a wider mass range and better resolving power is the SUrface Dust Analyzer (SUDA)[29] on board the Europa Clipper spacecraft, which aims to study

Received: October 8, 2022
Accepted: January 30, 2023
Published: February 8, 2023

https://doi.org/10.1021/acs.analchem.2c04429
Anal. Chem. 2023, 95, 3621−3628

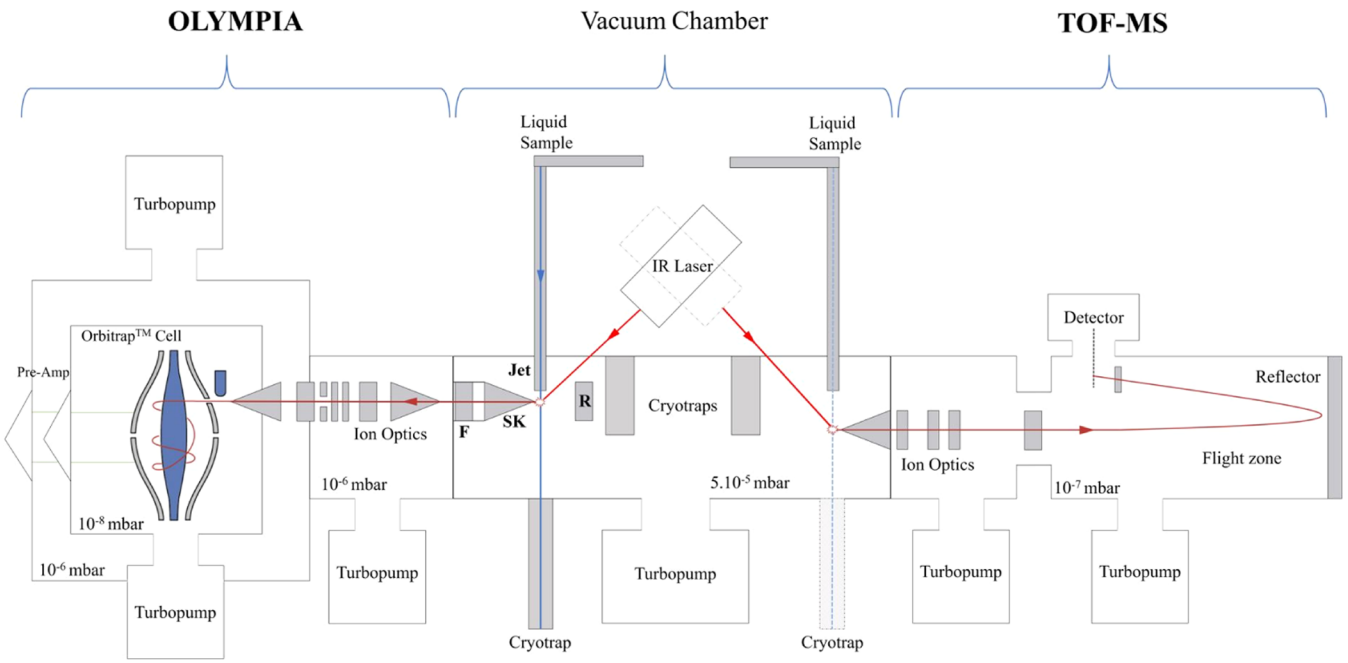

Figure 1. Schematic of the current setup at the FU Berlin laboratory. OLYMPIA has been connected in parallel to the TOF mass spectrometer. R: repeller, SK: skimmer, and jet: water beam high voltage (HV). The laser has been placed above the setup for illustration reasons; in reality the laser shot hits the water beam perpendicularly to both ion optics.

Jupiter's icy moon Europa.[2] The mass resolution of SUDA is 150−300 $m/\Delta m$ in the range of m/z 1−500 and will be able to measure both cationic and anionic mass spectra. Further in the future, TOF detectors with even higher performance are proposed, like ENIJA[30] (ENceladus Icy Jet Analyzer), which is planned to have a mass range of up to 2000 m/z, with a 1000−2000 $m/\Delta m$ mass resolution.[31,32] To simulate hypervelocity dust impacts, mass analyzers can be coupled with dust accelerators and reach spacelike impact velocities that are typically of the order of 10 km/s for μm-sized dust grains.[33] However, the acceleration of μm-sized ice grains to such an impact speed is not yet feasible.[34] Instead, to mimic in the laboratory icy grains mass spectra, the laser-induced liquid beam ion desorption (LILBID) technique is used.[35] Indeed, the LILBID technique is able to reproduce the ionization process of hypervelocity ice grain impacts. The ability to simulate the ice grains from a plume or ejected from the surface of an icy moon is a great asset, which has been extensively and successfully used to characterize the habitability of Enceladus with CDA data.[15,16,27,28] Using a pulsed infrared laser, a μm-sized water beam is subjected to a fast laser-induced dispersion, resulting in gas-phase ions. Relevant materials, such as minerals or organics, can be dissolved or finely dispersed in the water beam and studied at different experimental parameters (*e.g.*, laser energy densities) that can be correlated to different ice grain impact speeds.[36] Initially, LILBID setups were coupled with a TOF mass spectrometer. At the FU Berlin laboratory, the setup can reach a mass resolution $m/\Delta m$ of around 600−800. The SUDA team is building a database[37] containing calibration mass spectra for impact ionization MS that will help for future data interpretation. Even with this laboratory setup, the mass resolution is not sufficient to resolve isobaric interferences and to allow an unambiguous determination of chemical species. To resolve such interferences, a high-resolution mass spectrometer is needed. Laboratory mass spectrometers with such a resolving power have already been developed; however, the constraints of the space environment do not allow a simple spatialization of all techniques. The size, weight, and energy consumption of the instrument present serious limitations. Among the high-resolution mass analyzers, the commercial Orbitrap by Thermo Fisher Scientific[38] could fulfill those criteria after adaptations. Using a quadro-logarithmic electrostatic ion trap (QLEIT), based on a so-called Kingdon trap,[39] this mass analyzer uses a Fourier transform detection method, which means the mass resolution increases with the acquisition time. Orbitrap is able to reach a mass resolution of up to 1 000 000 at m/z below 300−400 within a 3 s detection time,[40] in an ultrahigh vacuum (10^{-10} mbar). A consortium of six laboratories[41] is currently developing the CosmOrbitrap, a space-ruggedized version of the Orbitrap mass analyzer plus its power supply electronics and data processing Fourier transform system for space applications. Coupled with a laser ablation ionization system, the CosmOrbitrap achieved mass resolution performances varying from 474 000 at m/z 9 to 90 000 at m/z 208 for a 830 ms signal duration.[42] The CosmOrbitrap is intended to be the mass analyzer of various laser ionization instruments currently under development for future planetary body missions.[43−45] In this work, we coupled the LILBID technique with a newly built laboratory Orbitrap-based mass spectrometer not intended for space applications, the Orbitrap anaLYzer MultiPle IonizAtion (OLYMPIA).[46] OLYMPIA was designed to be easily coupled with different ionization techniques, either continuous or pulsed. The coupling with the LILBID setup will allow a study of ice grain analogue samples with high mass resolution. The recorded mass spectra are intended to be included in the LILBID database built for SUDA's calibration in the Europa Clipper mission and future icy moons missions. With the current LILBID-TOF setup, isobaric interferences prevent an unambiguous peak assignment and an agnostic interpretation of the results. For this reason, hypervelocity detectors like

https://doi.org/10.1021/acs.analchem.2c04429
Anal. Chem. 2023, 95, 3621−3628

SUDA will greatly benefit from a high-resolution laboratory database for the data interpretation.

EXPERIMENTAL SECTION

OLYMPIA Mass Spectrometer. OLYMPIA uses a commercial quadro-logarithmic electrostatic ion trap (QLEIT), an Orbitrap cell from Thermo Fisher Scientific. Thanks to a modular design, the ionization technique of OLYMPIA is easily interchangeable. Although it is a great challenge to use direct injection, to compact its design, our current setup does not feature a C-trap module, usually included in commercial instruments.[47] A C-trap is used as an intermediate storage device from which the ions are injected into the Orbitrap, in a spatially and energetically well-defined ion packet. As a first stage of development, OLYMPIA has been used with an electron ionization (EI) ion source to test each subsystem and to study gas samples relevant for planetary atmospheres.[46] OLYMPIA is composed of a commercial D30 cell from Thermo Fisher, which is around 60 mm long for 40 mm diameter. A detailed description of the Orbitrap functioning can be found in the literature.[38,40,47,48] Briefly, after focus, the ions are injected into the trap through a millimetric aperture and are squeezed electrodynamically around the central electrode.[48] The timing for the squeezing is relative to the laser pulse and is triggered a few microseconds after the ionization. The trapped ions oscillate in the cell with a frequency defined by the trap parameters and their m/z value. A large window of frequency can be measured during a single acquisition. As the frequency difference between heavy ions is lower than light ions, the mass range of an Orbitrap is not linear and increases with the m/z ratio. The maximum mass range is defined by a minimum to maximum mass ratio of 30. The mass range in this work is around 10 to 300 u. The detected signal is amplified by a preamplifier and converted by an analogue-to-digital convertor (ADC). Finally, using a discrete or fast Fourier transformation (DFT and FFT, respectively), the oscillation frequency of the ions is obtained.[47]

For this work, we coupled OLYMPIA with a LILBID setup at the FU Berlin to simulate hypervelocity ice grain impacts and measure their composition with high mass resolution. We adapted the LILBID setup presented in Charvat et al. (2007).[35]

Coupling in Parallel of the TOF-MS. OLYMPIA has been implemented in the LILBID-TOF setup on the opposite side of the main vacuum chamber (Figure 1). This configuration offers the possibility to use both methods to measure the same samples, allowing a direct data comparison. Switching from one mass spectrometer to the other can be done simply by changing the laser position.

Laser and Optics. We use a pulsed IR laser (Opolette HE 2731, OPOTEK) at 2840 nm with a 7 ns pulse width at a 20 Hz repetition rate. The laser energy is around 2 mJ per pulse. The measurement time for the Orbitrap usually spans a few hundred milliseconds. To minimize in the Orbitrap charge effects and radio frequency (RF) noise, the Q-Switch of the laser is fired only once per second. The triggering and synchronization with the Orbitrap cell are ensured by a CompactRIO controller (cRIO-9023, National Instruments). The laser radiation is steered by gold-coated mirrors and focused on the liquid beam with two CaF_2 AR-coated lenses through a CaF_2 window. We measured the spatial distribution of the laser energy on the OLYMPIA side using the knife-edge method[49] and estimated the laser power density at the water beam to be about 950 MW/cm^2, a value close to that used in the LILBID-TOF setup (~1150 MW/cm^2).[36]

Liquid Beam. Using an HPLC pump (model 300c, Gynkotek) and a nozzle mounted on a 3-axis manipulator, a water beam with a diameter of 20 μm and a flow rate of typically 0.2−0.3 mL/min is created. The quartz nozzle of the standard LILBID-TOF setup has been replaced by a metallic nozzle, which can easily be set to a defined electric potential (see below).

Ion Optics. The electrodynamic squeezing by the Orbitrap requires defined kinetic energy[48] (KE) distribution of the ions. If so, both the number of trapped ions and their lifetime inside the cell increase, and thus the data quality improves (*e.g.*, mass resolution or reproducible conditions for quantitative measurements). As already mentioned, in commercial Orbitrap instruments, the size and KE distribution of ion packets injected into the Orbitrap are guaranteed by the C-Trap module. Because of the absence of C-Trap in our design, the control of the KE must be accomplished with the ion optics only. In our setup, the measuring potential of the Orbitrap central electrode is −3500 V; for this value, the optimal KE for the ions to be captured is around 1100 eV. At the location of ion generation, the ion optics creates an electrostatic field that accelerates the ions to this desired KE. The surroundings of the water beam have been modified compared to the LILBID-TOF source, which does not require an electrostatic field at the ionization site. In addition to the metallic nozzle, a repeller electrode has been added to push the ions toward the Orbitrap and a potential can be applied on the skimmer close to the water beam (Figure 1). A fourth electrode is placed after the skimmer. A high voltage of up to 2000 V relative to the electrical ground can be applied on each of these electrodes with HV power supplies (iseg Spezialelektronik). It is worth noting that using the LILBID-TOF source, the ions fly from the water beam toward the extraction region of the TOF in a field-free environment and are then accelerated by applying a short HV pulse to the TOF electrodes. By changing the delay time between ion generation (*i.e.*, laser pulse) and this commutation, different ions can be selected. While at short delay times fast ions with smaller masses are selected, at longer delays, heavier ions can be detected. The main difference with the LILBID-OLYMPIA source with the current settings is that the ions are not allowed to fly freely but are immediately accelerated to a rather high KE. However, if required, the timing for the Orbitrap central electrode can be adjusted to analyze, *e.g.*, the trailing part of the ion distribution. A postacceleration is also possible by switching the potentials after the ion's creation. After the first four electrodes, the ion beam is focused into a seven-element manifold/stack. It consists of four circular lenses that allow focusing or defocusing according to the voltage polarity applied and three half-circular elements for deflection of the ion beam (Figure 1).

Electron Multiplier for Alignment. To adjust and optimize the ion optics settings, an electron multiplier (DeTech 2300) has been placed behind the Orbitrap and measures the ions going through the cell. The output signal of this detector allows visualization of the ion packet duration, intensity, and velocity.

Multistage Vacuum Design. As mentioned above, the lifetime of the ions is one of the key parameters for high-resolution measurements. The lifetime of ions trapped inside a

https://doi.org/10.1021/acs.analchem.2c04429
Anal. Chem. 2023, 95, 3621−3628

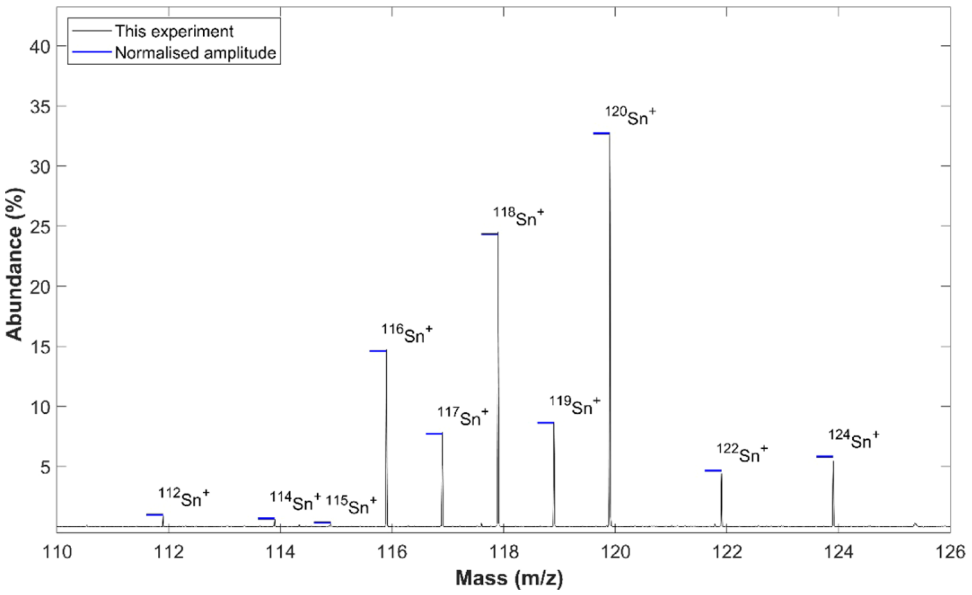

Figure 2. Tin mass spectrum recorded with the setup. The acquisition time for this plot is 50 ms. Then, 28 mass spectra are coadded and averaged. The horizontal lines represent the theoretical abundance value of each isotope (see Table 1) normalized to the major isotope ($^{120}Sn^+$) intensity.

Table 1. Theoretical Properties of Tin from the NIST Standard[52] and the Measured Values from This Work[a]

isotope	mass (theoretical)	abundance (theoretical)	mass accuracy (ppm)	mass resolution (FWHM)	SNR	intensity deviation (50 ms)	intensity deviation
^{112}Sn	111.9048 u	0.97%	0.4	42 339	41	−19.4 ± 5.5%	−6.8 ± 10.5%
^{114}Sn	113.9028 u	0.66%	1.3	44 908	22	−25.2 ± 6.2%	−17.9 ± 12.8%
^{115}Sn	114.9033 u	0.34%	−2.1	41 017	9	−17.5 ± 9.4%	−15.8 ± 21.3%
^{116}Sn	115.9017 u	14.54%	1	40 348	599	−5.8 ± 2.4%	+ 3.1 ± 6.8%
^{117}Sn	116.9030 u	7.68%	−0.9	40 593	315	−3.2 ± 2.5%	+ 1.4 ± 7.1%
^{118}Sn	117.9016 u	24.22%	0.0	40 653	1014	−2.6 ± 1.8%	+ 5.0 ± 6.2%
^{119}Sn	118.9033 u	8.59%	3.3	40 644	338	−6.4 ± 1.8%	+ 3.3 ± 4.9%
^{120}Sn	119.9022 u	32.58%	calibrant	41 145	1257	calibrant	calibrant
^{122}Sn	121.9034 u	4.63%	−0.7	41 157	153	−3.0 ± 2.2%	−11.4 ± 5.6%
^{124}Sn	123.9053 u	5.79%	0.6	41 136	189	−3.5 ± 2.5%	−9.3 ± 4.9%

[a]Intensity deviation shows the center of the normal distribution fit and the 1-σ uncertainties (see Figure S2 for the histograms and fit plots). Unless indicated otherwise, values are for 250 ms mass spectra.

commercial Orbitrap is usually several seconds[50] and the vacuum of the order of 10^{-10} mbar. To minimize collisions with the neutral background molecules in our experiments, a four-stage vacuum system has been designed. First, in the main vacuum chamber, a turbomolecular pump (STP-iS2207, Edwards Vacuum) evacuates the water beam chamber. Two liquid nitrogen-cooled cryotraps are used to efficiently pump out the water vapor. Another cryotrap is used as a liquid beam dump. The resulting pressure in the main chamber is around 5×10^{-5} mbar. Downstream the main chamber, ion optics, OLYMPIA chamber, and the Orbitrap cell are interfaced through differential pumping walls with apertures of less than 1 mm in diameter. Each of these three stages is pumped with a turbomolecular pump (HiPace 80 & HiPace 300, Pfeiffer Vacuum). The resulting pressure in the cell during measurements is typically $\sim 10^{-8}$ mbar, which is a rather high value for Orbitrap measurements. Previous studies have shown[41,51] that the mass resolution starts to deteriorate by the neutral background gas at pressures above 1×10^{-8} mbar. We thus expect a difference between the measure, and theoretical mass resolution of the measurements.

RESULTS AND DISCUSSION

Tin Study Results and Performances. After a successful parallel mechanical integration of the OLYMPIA setup on the LILBID-TOF at the FU Berlin laboratory, the first steps were to control the correct alignment of the ion source with the ion optics and the Orbitrap. To ease this step and those of ion optics precalibration and timings, we first ionized a metal wire, as higher production of ions under laser−surface interaction is obtained than under the laser−liquid performed by LILBID. We analyzed a tin wire with 99.98% purity (Figure 2). The 10 stable isotopes of tin, which present an abundance variation of up to 3 orders of magnitude, allow to estimate the relative isotopic abundance (RIA) accuracy of the setup. The tin measurements also give a first idea of the setup's overall performances, such as mass resolution, mass accuracy, or detection limit.

The lifetime of ions in the Orbitrap cell is limited by several factors such as geometry imperfections, collision with a neutral background, or HV instabilities during the measurement time.[48] Moreover, the free induction decay transient of each isotope through time can be different, as less abundant ions are more affected by space charge effects than isotopes in higher

https://doi.org/10.1021/acs.analchem.2c04429
Anal. Chem. 2023, 95, 3621−3628

proportions.[53] The less abundant ions are therefore more likely to be repelled from a stable orbit, inducing an underestimation of these species. For the same reason, minor species will also be more impacted by the field imperfections. Overall, the deviation of quantitative measurements is affected over time, even for major ions, resulting in increasing errors over time. However, to improve the RIA accuracy, we can choose to analyze a short fraction (~50 ms) of the measured signal and calculate the deviation before it is too much disturbed by space charge effects or imperfections in the electrostatic field. The same data can then be analyzed with a longer signal duration (a few hundreds milliseconds) to greatly improve the mass resolution. For this study, we show the mass resolution and mass accuracy for a 250 ms signal. The method for ion count quantification and isotopic comparison is explained in the Supporting Materials. Briefly, the total ion count for one isotope is the area under the curve of its peak, starting at 10% peak height (Figure S1). Each isotope ion count is normalized to the major $^{120}Sn^+$. The deviation errors are gathered in histograms on which a normal distribution fit is applied. The maximum of the fit is the mean error, and the 1-σ value is the confidence interval for 68.2% of the data (Figure S2). The deviation between the measured and theoretical abundances is shown for both a 50 ms signal and a 250 ms signal (Table 1). The different tin isotope abundances are shown in Table 1. The recorded mass spectrum is shown in Figure 2. To improve statistics and reduce the noise, we coadded and averaged 28 single mass spectra, selecting mass spectra only with high signal intensity. On each raw data recorded with the Orbitrap, we apply a Hann function-shaped window[54] to minimize spectral leakage and a 32 times zero-padding[55] to increase the discrete resolution. We managed to detect all 10 major isotopes of Tin, even the lowest abundant one $^{115}Sn^+$ (0.34%), which brings the dynamic range of the setup with the current settings to about 10^3. The intensity deviation of the more abundant isotopes (>4%) is on average −4% (± 2.2%). For the lowest abundant isotopes (<1%), the deviation is higher, around −20%. With a 250 ms signal, the intensity deviations become more variable. The peaks are all around 40 000 mass resolution (FWHM) with a highly precise mass accuracy of a few ppm (Table 1). The theoretical mass resolution at the mass of tin for a 250 ms mass spectra is around 80 000 without a function-shaped window and about half this value[56] when using a Hann window as we do in this work. As we do not use an outgassing sample, the pressure in the cell is around 2×10^{-9} mbar. The results in Table 1 reach this theoretical mass resolution, demonstrating that the setup is highly efficient. It is worth noting that the mass resolution values of Table 1 correspond to mass spectra that have been averaged and resampled. The measured mass resolution may therefore be slightly above the theoretical one. The mass resolution for unaveraged mass spectra is at 95% of the theoretical.

On a short signal duration (50 ms), the intensity quantification has only a few percent deviation. We observe a greater deviation for low abundant ions due to space charge effects, which have a larger effect on low abundant ion packets compared to major isotopes.[53] Over time, the decrease of each ion intensity can be different due to neutral background or imperfections in the electrostatic field, resulting in an increasing deviation error between 50 and 250 ms.

Water Beam Results and Performances. The study of the tin wire has confirmed the success of the mechanical integration and allowed us to do a precalibration of the ion optics potentials and commutation timings. We then analyzed purified water ionized with the LILBID technique. We successfully measured water ions ($H_{2\text{-}3}O^+$) with OLYMPIA. A mass spectrum is shown in Figure 3. The current results are

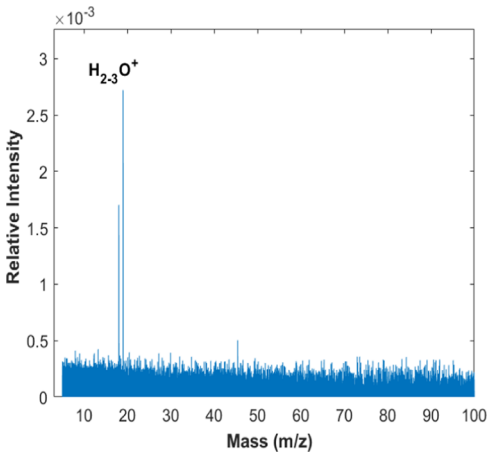

Figure 3. H_2O^+ and H_3O^+ single mass spectrum recorded with the LILBID-OLYMPIA setup. The acquisition time for this spectrum is 80 ms.

presented with a signal duration of 80 ms. Both H_3O^+ and H_2O^+ ions stand out from the noise level with an SNR of around 20 and 10, respectively. By coadding and averaging only a few mass spectra, we can significantly reduce the noise level and reach SNR ratios of about 100 (Figure S3).

The lifetime of ions in the cell was sufficient to reach the high mass resolution expected with an Orbitrap. As shown in Figure 4, the recorded mass resolution is above 25 000 $m/\Delta m$ for both peaks, for an 80 ms mass spectrum. The theoretical mass resolution at the mass of water and for this FFT duration and the use of a Hann window is around 31 000 $m/\Delta m$. As for the tin mass spectra, the measured mass resolution is much close to the theoretical value. In addition, the mass accuracy is also in the same range as with the tin wire data, with 11 ppm on the single mass spectrum presented, but which is usually below 3 ppm for an averaged mass spectrum.

Discussions of the Water Beam Experiments. To characterize the lifetime of ions and the maximum acquisition time, the signal can be divided into different slices through time and analyzed separately. This helps to follow the decrease of the signal through time. Figure 5 presents the averaged SNR during the measurements. The major species, H_3O^+, starts with an SNR of around 30. The amplitude shows a dip of around 75 ms. This could be attributed to variations or an improper optimization of the Orbitrap electrode (*i.e.*, central or deflection) potential during the acquisition time, although this point is the subject of further work. With such variations, the ions would drift away from their original oscillation frequency, hence the amplitude diminution. After a potential stabilization, the H_3O^+ ions return to their initial frequency and the SNR increases again. The SNR then steadily decreases, and an SNR of around 5 can still be observed at 250 ms. The H_2O^+ ions are less abundant with the current setting; at the beginning of the signal, the SNR is around 10 and decreases faster than H_3O^+ ions. After 150 ms, the signal is too low to be measurable.

On single mass spectra, H_3O^+ ions can be detected up to 500 ms in the cell, reaching a mass resolution of around

https://doi.org/10.1021/acs.analchem.2c04429
Anal. Chem. 2023, 95, 3621−3628

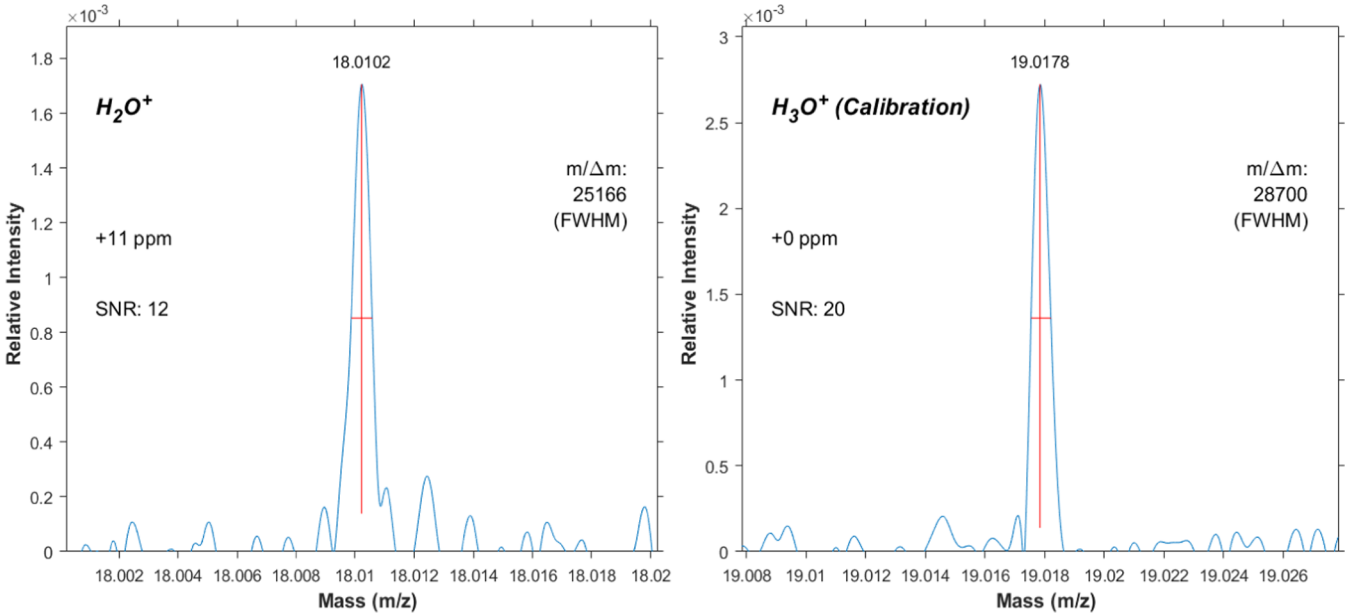

Figure 4. Zoom on the H_2O^+ and H_3O^+ peaks shown in Figure 3. The mass resolution, the mass accuracy, and the SNR are shown on the plot. The mass resolution is calculated using the full width at half maximum (FWHM). The base of the vertical line represents the noise level calculated by averaging the positive values of the mass spectra; the features around the peaks are therefore noise artifacts. The horizontal line represents the width at half maximum. To increase the peak shape quality, we applied a zero-filling (4 times) and a Hann function-shaped window.

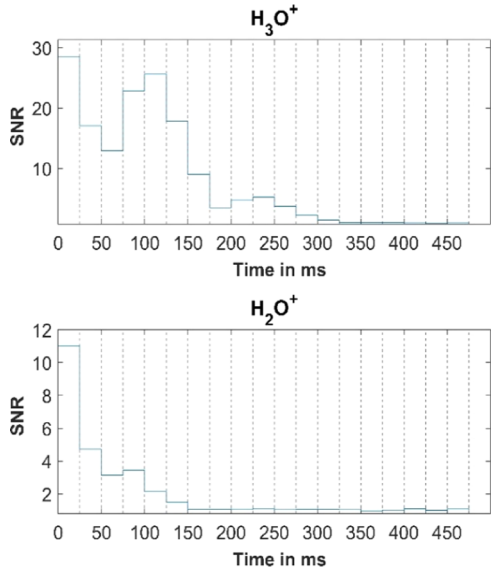

Figure 5. Signal to noise ratio for H_3O^+ and H_2O^+ through time. Each slice represents the average SNR value of about 40 spectra. The total signal duration is 500 ms and is cut into 20 slices of 25 ms.

150 000 FWHM (Figure S3). H_2O^+ ions are, for now, destabilized after 80 ms, and a longer signal duration would not increase the data quality for this chemical species.

Laser Energy to Analogue Velocity. As shown by Klenner et al. (2019), the laser energies used during the experiments can be translated to impact speeds of spaceborne icy grains onto metal targets. By comparing the recorded OLYMPIA spectra with the LILBID-TOF spectra, we find that the spectral appearances match those of ice grains at impact speeds of 15−18 km/s.36 This demonstrates the proof-of-concept objective of this work. Future experiments will aim to simulate lower impact speeds, which will require a modification of the current experimental setup.

CONCLUSIONS AND OUTLOOK

We successfully coupled OLYMPIA, a newly built Orbitrap-based mass spectrometer device to an LILBID setup, the reference technique for the simulation of hypervelocity ice grain mass spectra. This unique device is now able to record high-resolution mass spectra of liquid water. The focusing of water ions from the adapted LILBID source to the OLYMPIA mass analyzer has been achieved, and the first recorded mass spectra show H_3O^+ and H_2O^+ peaks, which look analogues to mass spectra of ice grains with the impact speed between 15 and 18 km/s measured with a CDA-type instrument. With sufficient SNR, the mass resolution of the mass spectra is usually between 80 and 95% of the theoretical mass resolution of an Orbitrap cell. This demonstrates the overall great performance of the setup. The lifetime of H_3O^+ ions in the trap can be up to 500 ms, allowing us to measure peaks with a mass resolution of around 150 000 $m/\Delta m$. H_2O^+ ions are destabilized earlier and survive for a shorter time period. Work is currently in progress on the setup to increase its performance and better stabilize the ion packet.

The tin isotopic study showed that the RIA deviation of OLYMPIA was deviated by less than a few percent from the theoretical value for isotopes with at least a few percent of abundance.

The LILBID-OLYMPIA setup has shown its ability to measure high laser energy mass spectra. Further work will now focus on producing and measuring water clusters, which appear at lower impact speeds in impact ionization data. To do so, we will first decrease the laser energy but also explore the effect of pulsing the electrodes of the ion optics and varying this delay time parameter, which we for now left aside. We will then dissolve inorganic and organic samples of interest in the liquid water and will be able to contribute to the SUDA database with high-resolution mass spectra.[37] In parallel, we are also exploring the impact of the electrostatic field in the ion source. By performing measurements on the LILBID-TOF setup with

https://doi.org/10.1021/acs.analchem.2c04429
Anal. Chem. 2023, 95, 3621−3628

the HV-compatible metal nozzle, we will be able to characterize the effects of the HV on the ionization and water clusters.

■ ASSOCIATED CONTENT

Supporting Information

The Supporting Information is available free of charge at https://pubs.acs.org/doi/10.1021/acs.analchem.2c04429.

Ion count quantification example. The area under the curve is calculated above the horizontal red lines, placed at 10% of the peak height (Figure S1); intensity deviation of tin isotopes (50 ms mass spectra) (Figure S2); and zoom on the H_3O^+ peak with a 500 ms acquisition time (Figure S3) (PDF)

■ AUTHOR INFORMATION

Corresponding Author

Arnaud Sanderink − *Laboratoire de Physique et Chimie de l'environnement et de l'Espace, UMR-CNRS 7328, 45071 Orléans, France; Institute of Geological Sciences, Freie Universität Berlin, 12249 Berlin, Germany;* orcid.org/0000-0001-5637-4579; Email: arnaud.sanderink@cnrs-orleans.fr

Authors

Fabian Klenner − *Institute of Geological Sciences, Freie Universität Berlin, 12249 Berlin, Germany;* orcid.org/0000-0002-5744-1718

Illia Zymak − *ELI-Beamlines, 252 41 Dolní Břežany, Czech Republic*

Jan Zabka − *J. Heyrovsky Institute of Physical Chemistry, Academy of Sciences of the Czech Republic, 182 00 Prague 8, Czech Republic*

Frank Postberg − *Institute of Geological Sciences, Freie Universität Berlin, 12249 Berlin, Germany*

Jean-Pierre Lebreton − *Laboratoire de Physique et Chimie de l'environnement et de l'Espace, UMR-CNRS 7328, 45071 Orléans, France*

Bertrand Gaubicher − *Laboratoire de Physique et Chimie de l'environnement et de l'Espace, UMR-CNRS 7328, 45071 Orléans, France*

Ales Charvat − *Institute of Chemical Technology, University Leipzig, 04103 Leipzig, Germany*

Bernd Abel − *Institute of Chemical Technology, University Leipzig, 04103 Leipzig, Germany;* orcid.org/0000-0001-6032-1680

Miroslav Polášek − *J. Heyrovsky Institute of Physical Chemistry, Academy of Sciences of the Czech Republic, 182 00 Prague 8, Czech Republic*

Barnabé Cherville − *Laboratoire de Physique et Chimie de l'environnement et de l'Espace, UMR-CNRS 7328, 45071 Orléans, France*

Laurent Thirkell − *Laboratoire de Physique et Chimie de l'environnement et de l'Espace, UMR-CNRS 7328, 45071 Orléans, France*

Christelle Briois − *Laboratoire de Physique et Chimie de l'environnement et de l'Espace, UMR-CNRS 7328, 45071 Orléans, France*

Complete contact information is available at: https://pubs.acs.org/10.1021/acs.analchem.2c04429

Notes

The authors declare no competing financial interest.

■ ACKNOWLEDGMENTS

The authors thank Dr. Alexander Makarov for valuable discussions about this work. A.S. thanks the French Space National Agency, the Centre National des Etudes Spatiales (CNES), as well as ERC Consolidator Grant 724908-Habitat OASIS for the funding of his Ph.D. The authors also gratefully acknowledge CNES for funding the instrumental development of OLYMPIA. This work was also supported by the Czech Science Foundation (grant no. 21-11931J). The authors are also grateful to M. Nezvedová for her help during the coupling campaign.

■ REFERENCES

(1) Grasset, O.; Dougherty, M. K.; Coustenis, A.; et al. *Planet Space Sci.* **2013**, *78*, 1−21.
(2) Howell, S. M.; Pappalardo, R. T. *Nat. Commun.* **2020**, *11*, No. 1311.
(3) Matson, D. L.; Spilker, L. J.; Lebreton, J. P. The Cassini/Huygens Mission to the Saturnian System. In *The Cassini-Huygens Mission*; Russell, C. T., Ed.; Springer: Netherlands, 2003; pp 1−58.
(4) Klein, H. P. *Rev Geophys.* **1979**, *17*, 1655.
(5) Carr, M. H.; Belton, M. J. S.; Chapman, C. R.; et al. *Nature* **1998**, *391*, 363−365.
(6) Thomas, P. C.; Tajeddine, R.; Tiscareno, M. S.; et al. *Icarus* **2016**, *264*, 37−47.
(7) Hsu, H. W.; Postberg, F.; Sekine, Y.; et al. *Nature* **2015**, *519*, 207−210.
(8) Lowell, R. P. *Geophys. Res. Lett.* **2005**, *32*, No. L05202.
(9) Hand, K. P.; Carlson, R. W.; Chyba, C. F. *Astrobiology* **2007**, *7*, 1006−1022.
(10) Parkinson, C. D.; Liang, M. C.; Yung, Y. L.; Kirschivnk, J. L. *Origins Life Evol. Biospheres* **2008**, *38*, 355−369.
(11) Hand, K. P.; Sotin, C.; Hayes, A.; Coustenis, A. *Space Sci. Rev.* **2020**, *216*, No. 95.
(12) Porco, C. C.; Helfenstein, P.; Thomas, P. C.; et al. *Science* **2006**, *311*, 1393−1401.
(13) Roth, L.; Saur, J.; Retherford, K. D.; et al. *Science* **2014**, *343*, 171−174.
(14) Postberg, F.; Schmidt, J.; Hillier, J.; Kempf, S.; Srama, R. *Nature* **2011**, *474*, 620−622.
(15) Postberg, F.; Kempf, S.; Hillier, J. K.; et al. *Icarus* **2008**, *193*, 438−454.
(16) Postberg, F.; Kempf, S.; Schmidt, J.; et al. *Nature* **2009**, *459*, 1098−1101.
(17) Teolis, B. D.; Perry, M. E.; Magee, B. A.; Westlake, J.; Waite, J. H. *J. Geophys. Res.: Space Phys.* **2010**, *115*, No. A09222.
(18) Hansen, C. J.; Esposito, L. W.; Colwell, J. E.; et al. *Icarus* **2020**, *344*, No. 113461.
(19) Niemann, H. B.; Booth, J. R.; Cooley, J. E.; et al. *IEEE Trans. Geosci. Remote Sens.* **1980**, *GE-18*, 60−65.
(20) Anderson, D. M.; Biemann, K.; Orgel, L. E.; et al. *Icarus* **1972**, *16*, 111−138.
(21) Niemann, H. B.; Atreya, S. K.; Bauer, S. J.et al. The Gas Chromatograph Mass Spectrometer for the Huygens Probe. In *The Cassini-Huygens Mission*; Russell, C. T., Ed.; Springer: Netherlands, 2003; pp 553−591.
(22) Balsiger, H.; Altwegg, K.; Bochsler, P.; et al. *Space Sci. Rev.* **2007**, *128*, 745−801.
(23) Kissel, J.; Altwegg, K.; Clark, B. C.; et al. *Space Sci. Rev.* **2007**, *128*, 823−867.
(24) Altwegg, K.; Balsiger, H.; Bar-Nun, A.; et al. *Sci Adv.* **2016**, *2*, No. e1600285.
(25) Auer, A.; Sitte, K. *Earth Planet Sci. Lett.* **1968**, *4*, 178−183.

(26) Srama, R.; Ahrens, T. J.; Altobelli, N.; et al. *Space Sci. Rev.* **2004**, *114*, 465−518.
(27) Postberg, F.; Khawaja, N.; Abel, B.; et al. *Nature* **2018**, *558*, 564−568.
(28) Khawaja, N.; Postberg, F.; Hillier, J.; et al. *Mon. Not. R. Astron. Soc.* **2019**, *489*, 5231−5243.
(29) Kempf, S.; Altobelli, N.; Briois, C.et al. In *SUDA: A Dust Mass Spectrometer for Compositional Surface Mapping for a Mission to Europa*, Abstract presented at: European Planetary Science Congress (EPSC); EPSC: Cascais, Portugal, September 9, 2014 https://meetingorganizer.copernicus.org/EPSC2014/EPSC2014-229.pdf.
(30) Srama, R.; Postberg, F.; Henkel, H.et al. In *ENIJA: Search for Life with a High-Resolution TOF-MS for In-Situ Compositonal Analysis of Nano- and Micron-Sized Dust Particles*, Paper presented at: EGU General Assembly; Vienna, Austria, 2015. https://meetingorganizer.copernicus.org/EGU2015/EGU2015-13456.pdf.
(31) Reh, K.; Spilker, L.; Lunine, J. I.et al. In *Enceladus Life Finder: The Search for Life in a Habitable Moon*, 2016 IEEE Aerospace Conference; IEEE, 2016.
(32) Mitri, G.; Postberg, F.; Soderblom, J. M.; et al. *Planet. Space Sci.* **2018**, *155*, 73−90.
(33) Mocker, A.; Bugiel, S.; Auer, S.; et al. *Rev. Sci. Instrum.* **2011**, *82*, No. 095111.
(34) Belousov, A.; Miller, M.; Continetti, R.; et al. *J. Am. Soc. Mass Spectrom.* **2021**, *32*, 1162−1168.
(35) Charvat, A.; Abel, B. *Phys. Chem. Chem. Phys.* **2007**, *9*, 3335.
(36) Klenner, F.; Postberg, F.; Hillier, J.; et al. *Rapid Commun. Mass Spectrom.* **2019**, *33*, 1751−1760.
(37) Klenner, F.; Umair, M.; Walter, S. H. G.; et al. *Earth Space Sci.* **2022**, *9*, No. e2022EA002313.
(38) Makarov, A. *Anal Chem.* **2000**, *72*, 1156−1162.
(39) Kingdon, K. H. *Phys Rev.* **1923**, *21*, 408−418.
(40) Denisov, E.; Damoc, E.; Lange, O.; Makarov, A. *Int. J. Mass Spectrom.* **2012**, *325*−*327*, 80−85.
(41) Briois, C.; Thissen, R.; Thirkell, L.; et al. *Planet. Space Sci.* **2016**, *131*, 33−45.
(42) Russo, R. *Talanta* **2002**, *57*, 425−451.
(43) Arevalo, R.; Selliez, L.; Briois, C.; et al. *Rapid Commun. Mass Spectrom.* **2018**, *32*, 1875−1886.
(44) Arevalo, R., Jr; Southard, A.; Danell, R.et al. In *Laser Desorption/Ablation Orbitrap Mass Spectrometry for the Exploration of Astrobiology Targets in the Next Decade*, Paper presented at: AGU Fall meeting, 2020. Online. https://agu.confex.com/agu/fm20/meetingapp.cgi/Paper/692087.
(45) Southard, A.; Hanna, A.; Kaplan, D.et al. In *Integration of a dual source linear ion trap and Orbitrap analyzer (AROMA) for in situ detection and characterization of biosignatures on Enceladus, Europa, and Ceres*, Paper presented at: AbSciCon; Atlanta, GA, USA, 2022.
(46) Zymak, I.; Sanderink, A.; Gaubicher, B.; Žabka, J.; Lebreton, J. P.; Briois, C. In *OLYMPIA - a compact laboratory Orbitrap-based high-resolution mass spectrometer laboratory set-up: Performance studies for gas composition measurement in analogues of planetary environments*, Poster presented at: EGU, 2021.
(47) Makarov, A.; Denisov, E.; Lange, O.; Horning, S. *J. Am. Soc. Mass Spectrom.* **2006**, *17*, 977−982.
(48) Hu, Q.; Noll, R. J.; Li, H.; Makarov, A.; Hardman, M.; Graham Cooks, R. *J. Mass Spectrom.* **2005**, *40*, 430−443.
(49) Skinner, D. R.; Whitcher, R. E. *J. Phys.* **1972**, *5*, 237−238.
(50) Grinfeld, D.; Stewart, H.; Skoblin, M.; Denisov, E.; Monastyrsky, M.; Makarov, A. *Int. J. Mod. Phys. A* **2019**, *34*, No. 1942007.
(51) Selliez, L. Optimisation de l'analyse de La Matière Organique à l'aide d'un Nouveau Spectromètre de Masse Basé Sur Le CosmOrbitrap Dans Un Contexte de Future Mission Spatiale. Dissertation, Université d'Orléans, 2018. http://www.theses.fr/2018ORLE2018.
(52) Berglund, M.; Wieser, M. E. *Pure Appl. Chem.* **2010**, *83*, 397−410.
(53) Hofmann, A. E.; Chimiak, L.; Dallas, B.; et al. *Int. J. Mass Spectrom.* **2020**, *457*, No. 116410.
(54) Harris, F. J. *Proc. IEEE* **1978**, *66*, 51−83.
(55) Marshall, A. G.; Verdun, F. R. *Fourier Transforms in NMR, Optical, and Mass Spectrometry: A User's Handbook*; Elsevier, 2016.
(56) Scigelova, M.; Hornshaw, M.; Giannakopulos, A.; Makarov, A. *Mol. Cell. Proteomics* **2011**, *10*, No. M111.009431.

https://doi.org/10.1021/acs.analchem.2c04429
Anal. Chem. 2023, 95, 3621−3628